Available online at www.sciencedirect.com
ScienceDirect
Journal of Crystal Growth 308 (2007) 105–109
JOURNAL OF CRYSTAL GROWTH
www.elsevier.com/locate/jcrysgro

The effect of growth time on the morphology of ZnO structures deposited on Si (1 0 0) by the aqueous chemical growth technique

D. Vernardou[a,b,c,*], G. Kenanakis[a,b,d], S. Couris[e,f], A.C. Manikas[f], G.A. Voyiatzis[f], M.E. Pemble[g], E. Koudoumas[a,h], N. Katsarakis[a,b,i]

[a]*Center of Materials Technology and Laser, School of Applied Technology, Technological Educational Institute of Crete, 710 04 Heraklion, Crete, Greece*
[b]*Science Department, School of Applied Technology, Technological Educational Institute of Crete, 710 04 Heraklion, Crete, Greece*
[c]*Department of Materials Science and Technology, University of Crete, 710 03 Heraklion, Crete, Greece*
[d]*Department of Chemistry, University of Crete, 710 03 Heraklion, Crete, Greece*
[e]*Department of Physics, University of Patras, 26504 Patras, Greece*
[f]*Institute of Chemical Engineering and High Temperature Chemical Processes (ICE-HT), Foundation for Research and Technology-Hellas (FORTH), 26504 Patras, Greece*
[g]*Tyndall National Institute, Lee Maltings, Prospect Row, Cork, Ireland*
[h]*Electrical Engineering Department, Technological Educational Institute of Crete, 710 04 Heraklion, Crete, Greece*
[i]*Institute of Electronic Structure and Laser, Foundation for Research and Technology-Hellas, P.O. Box 1527, Vassilika Vouton, 711 10 Heraklion, Crete, Greece*

Received 16 May 2007; received in revised form 11 July 2007; accepted 16 July 2007
Communicated by S. Uda
Available online 22 July 2007

Abstract

This paper examines the growth of ZnO structures on Si (1 0 0) using the aqueous chemical growth (ACG) technique for deposition times of between 1 and 40 h. It is found that ZnO grown using zinc nitrate hexahydrate ($Zn(NO_3)_2 \cdot 6H_2O$) and hexamethylenetetramine (HMTA) as precursors at 95 °C exhibits single-phase wurtzite ZnO crystal structure. The shape and the dimensions of the structures were found to depend on the growth time. The results are discussed in terms of kinetic studies carried out in correlation with the different deposition periods.

Keywords: A2. ACG; A2. Deposition time; A2. Growth mechanism; B1. ZnO

1. Introduction

ZnO is a well-known compound suitable for a wide variety of interesting applications in photonic crystals [1], photodetectors [2], varistors [3], surface acoustic devices [4], sensors [5] and solar cells [6]. Furthermore, it is very important for low-voltage and short wavelength electro-optical devices such as light emitting diodes and diode lasers due to its wide band gap (3.37 eV) and large exciton binding energy of 60 meV [7].

ZnO has a hexagonal (wurtzite) crystal structure with lattice parameters α and c in a ratio of $c/\alpha = 1.633$ [8]. The Zn atoms are tetrahedrally coordinated to four O atoms, where the Zn d-electrons hybridize with the O p-electrons.

Diverse morphologies of ZnO structures have been synthesized by various dry processes such as RF-sputtering [9], pulsed laser deposition (PLD) [10], molecular beam epitaxy (MBE) [11], thermal evaporation [12] and chemical vapour deposition (CVD) [13] as well as wet processes including electro-deposition [14], spray pyrolysis [15], sol–gel [16] and aqueous chemical growth (ACG) [17–19].

*Corresponding author. Department of Materials Science and Technology, University of Crete, School of Applied Technology, 710 03 Heraklion, Crete, Greece. Tel.: +30 2810 379895; fax: +30 2810 379845.
E-mail address: dvernardou@stef.teiher.gr (D. Vernardou).

0022-0248/$ - see front matter © 2007 Elsevier B.V. All rights reserved.
doi:10.1016/j.jcrysgro.2007.07.032

ACG is an advantageous and simple technique, requiring non-expensive equipment and non-toxic reagents, while the remaining by-products are non-hazardous. Moreover, the size and shape of the structures grown by this technique can be controlled by adjusting the growth parameters such as concentration of solution, reagents stoichiometry, pH and temperature [20,21].

In this report, we present kinetic data, which demonstrate possible mechanisms occurring during the ZnO growth. The effect of growth time on structural and morphological characteristics of samples is considered.

2. Experimental section

The growth of ZnO on Si (1 0 0) was performed by ACG, using $Zn(NO_3)_2 \cdot 6H_2O$ and hexamethylenetetramine (HMTA) as precursors. Just before deposition, all substrates were ultrasonically cleaned with propanol, acetone, MilliQ H_2O (18.2 MΩ cm at 25 °C) and dried with N_2. In a typical procedure for 50 ml of 10^{-2} M solution, $Zn(NO_3)_2 \cdot 6H_2O$ was first stirred with MilliQ H_2O and then HMTA was added under continuous stirring for another 15 min for 1:1 molar ratio. Finally, the solution was placed in Pyrex glass bottles with polypropylene autoclavable screw caps, with the substrate placed on the top of a microscope glass stand. The bottles were heated in a regular laboratory oven at a constant temperature of 95 °C for various deposition times of 1, 2, 5, 15, 20, 30 and 40 h. After each induction period, the samples were thoroughly washed with MilliQ H_2O, in order to eliminate any residual salts, and dried in air at a similar temperature (95 °C) [22].

X-ray diffraction (XRD) measurements were performed using a Rigaku (RINT 2000) Diffractometer with Cu Kα X-rays operating at 40 kV, 178 mA for $2\theta = 30.00-75.00^\circ$ and step size $0.02^\circ\,s^{-1}$. All peak positions and diffraction intensities were found to match with database reference spectra, JCPDS card file no. 36-1451, and the corresponding lattice constants were calculated using the 'ChekCell' software [23]. Raman measurements were carried out using a T-64000 model of Jobin Yvon (ISA-Horiba group), with the 514.5 nm line of an air-cooled Ar^+ laser (Spectra-Physics 163-A42) operating at ~2 mW power for an integration time of 300 s and a wavenumber range of 240–840 cm^{-1}. Scanning electron microscope (SEM) was performed with a JEOL JSM-840 electron microscope. Fourier transform infrared spectroscopy (FTIR) measurements were carried out using a Bruker IFS 66v/S spectrometer at a resolution of 2 cm^{-1} and sample scan time as well as background scan time of 32 scans for all samples. The measurements were carried out in the mid-IR region (350–4500 cm^{-1}) using KBr as the beamsplitter. For consistency, each characterization method was performed on at least three samples, prepared under the same conditions, and on various positions on the sample.

3. Results and discussion

The aim of these experiments was to study the influence of the deposition time on the growth of ZnO structures and examine its growth mechanism through kinetic data. For a range of deposition times up to 40 h and using a stoichiometric 1:1 ratio of $Zn(NO_3)_2 \cdot 6H_2O$:$C_6H_{12}N_4$ in a 10^{-2} M solution at 95 °C, the growth of single-phase ZnO was achieved. The deposited ZnO samples were white in colour over the whole area of the substrate, for all deposition conditions. Moreover, samples grown for longer deposition times appeared to have better adhesion, passing the Scotch tape test. Finally, they were observed to be stable in air for over 6 months.

Fig. 1 shows the XRD patterns of ZnO deposited on Si (1 0 0) for 1, 15 and 40 h. The 'patterns' are consistent with the wurtzite ZnO hexagonal P6(3)mc structure and present all the characteristic peaks and Miller indices with lattice constants of $a = 3.2504$ Å and $c = 5.2055$ Å. It is important to note that the same pattern was observed for all deposited ZnO samples that gave sufficient number of reflections to allow the calculation of the cell parameters. The Si (1 0 0) peaks are also indicated in Fig. 1, exhibiting a trend for decreased intensity and full-width at half-maximum (FWHM) as the deposition time increases, possibly due to the increase of the coverage of the substrate surface. The XRD patterns were found to be the same all

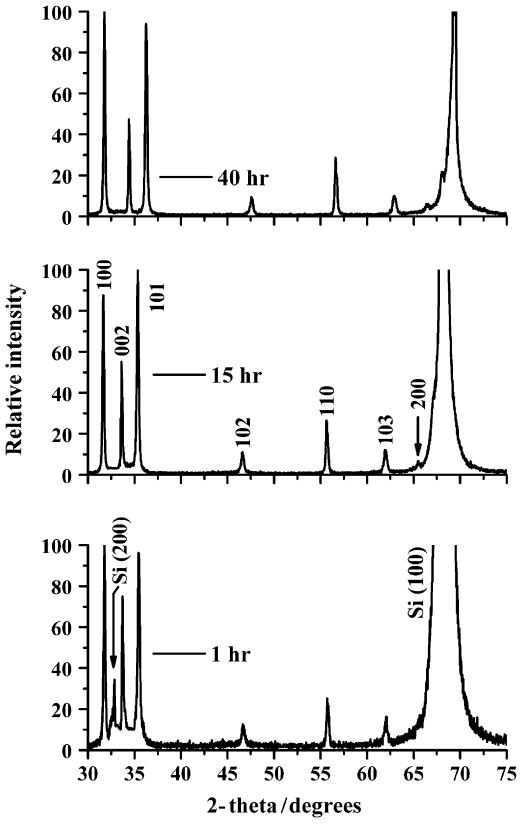

Fig. 1. XRD analysis of ZnO grown by ACG on Si (1 0 0) using 10^{-2} M solution of $Zn(NO_3)_2 \cdot 6H_2O$ and HMTA at 95 °C for deposition times of 1, 15 and 40 h.

along the surface of all samples, i.e. no variations in the phase as a function of position on the substrate were observed.

Fig. 2(a) shows the Raman spectrum of ZnO grown on Si (1 0 0) for a deposition period of 15 h. The observed phonon frequencies, indicating the presence of ZnO according to the literature [24,25], are: 332 cm^{-1} (multiple-phonon scattering processes), 379 cm^{-1} (A_1(TO)), 410 cm^{-1} (E_1(TO)), 437 cm^{-1} (E_2(high)) and 582 cm^{-1} (E_1(LO)), while the peak at 520 cm^{-1} is related to Si [26]. Among these peaks, the E_2(high) mode at 437 cm^{-1}, having the strongest intensity, corresponds to the band characteristic of the wurtzite phase [27]. Therefore, the recorded Raman spectrum clearly demonstrates that the composed ZnO has hexagonal wurtzite structure of good crystal quality, a result which is in agreement with the XRD analysis. Similar peaks were observed for longer deposition periods, at least up to 30 h, suggesting that, as noted earlier, single-phase of ZnO was the predominant product. On the other hand, the Raman spectrum recorded after 40 h deposition (Fig. 2(b)) showed similar peaks to the spectra obtained for the other samples, but broadened and with no clear evidence of vibrational contributions at 332, 379, 410 and 582 cm^{-1}. This may be possibly due to the presence of structures of different shape and dimensions, since there is no indication of defects, from either XRD [28] or Raman spectroscopy [29], coming from impurities such as $Zn(OH)_2$. As is demonstrated later in this paper, growth for longer periods does indeed results in a change in the morphology. The accompanying change in light scattering characteristics could be responsible for the degradation in the Raman signal observed although this remains to be unequivocally determined. Therefore, it is very interesting to note that for the longer growth periods studied (40 h), the crystalline quality of the deposited structures was observed to become slightly poorer (weaker and broader peaks), a behaviour not clearly observed in the XRD results since the latter technique is less sensitive than the Raman spectroscopy.

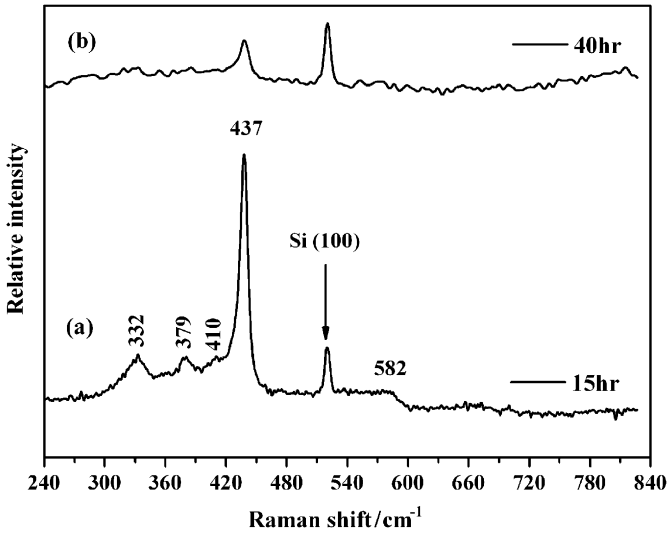

Fig. 2. Raman spectra of ZnO grown by ACG on Si (1 0 0) using 10^{-2} M solution of $Zn(NO_3)_2 \cdot 6H_2O$ and HMTA at 95 °C for deposition times of 15 (a) and 40 h (b).

SEM images of the ZnO structures deposited on Si (1 0 0) are shown in Figs. 3(a)–(c), for deposition times of 1, 15 and 40 h, respectively. A mixture of rods and flower-like architectures can be seen in all cases, while the exact shape and dimensions of the structures depended on the growth time. For short growth periods (Fig. 3(a)), sponge-like structures with mean diameter in the range of 2-4 μm are indicated, together with rods having diameter and length of approximately 1 and 10 μm, respectively. Furthermore, only a partial coverage of the substrate area could be

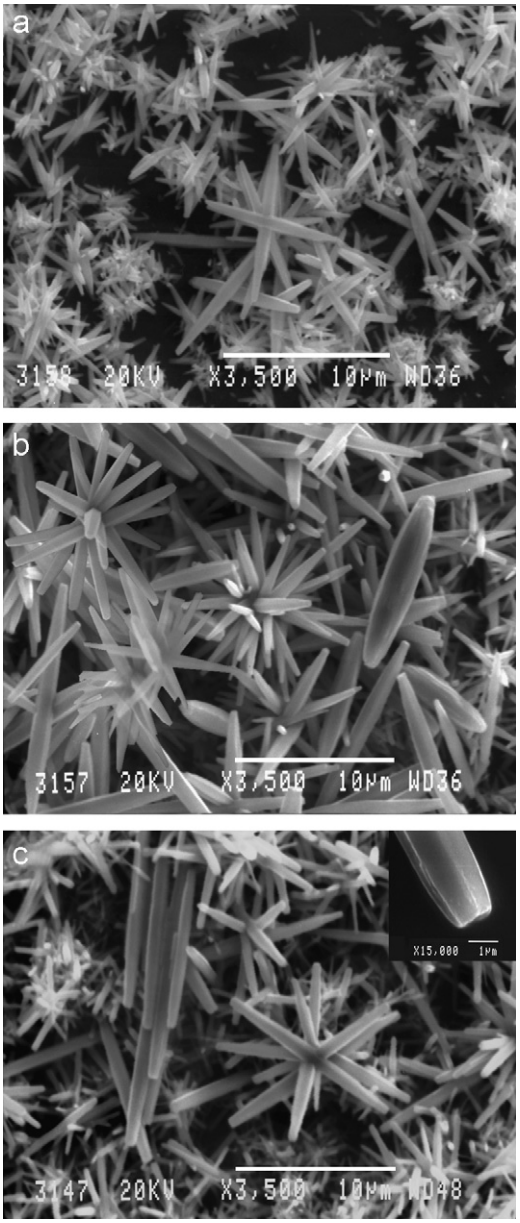

Fig. 3. SEM images of ZnO deposited on Si (1 0 0) by ACG using 10^{-2} M solution of $Zn(NO_3)_2 \cdot 6H_2O$ and HMTA at 95 °C, for deposition times of 1 (a), 15 (b) and 40 h (c). The line is equal to 10 μm. In the inset of (c) the hexagonal shape of the ZnO rods is observed, the line is equal to 1 μm.

achieved, consistent with the fact that in this regime we were examining the initial stages of the growth. For growth times in the range 10–30 h, well-formed flower-like structures with a diameter of about 7–8 μm predominate. In addition, a few single rods are also observed, having similar length as those grown for shorter times but slightly larger diameter (approximately 2 μm), (Fig. 3(b)). Furthermore, the coverage of the substrate area is significantly increased, i.e. from 40% for 1 h growth up to 60% for 15 h. Overall, ZnO flower-like architectures are mainly observed for growth times of between 1 and 30 h, the only difference being the size of the structures and the coverage of the substrate area. In contrast, the morphology of the 40 h samples was found to be different, showing flower-like architectures and single rods of significantly different sizes as well as a different way of 'distribution' with each other (Fig. 3(c)). This morphology change could be connected with the loss of some spectral features and the broadening of the peaks observed by Raman spectroscopy (Fig. 2). This behaviour may be due to the different growth mechanisms taking place for deposition times longer than 30 h, which will be discussed later. In any case, all grown structures consisted of hexagonal cross-section rods (inset of Fig. 3(c)), implying the occurrence of wurtzite ZnO crystal structure, an observation consistent with XRD (Fig. 1) and Raman spectroscopy (Fig. 2).

Fig. 4 presents the IR spectra of the 1 h and the 40 h samples, as well as the Si (1 0 0) substrate used for the deposition. The analysis of the spectra and the interpretation of the bands were based on data presented in the literature. The spectrum of the Si (1 0 0) substrate exhibits two characteristic peaks at 604 cm^{-1} (band A) and 1100 cm^{-1} (band B), which are allocated as the Si–Si vibration and the Si-O-Si mode correspondingly [30]. They can both be related to the formation of SiO_2 on the surface of the wafer after its exposure in air. The spectrum of the 1 h sample exhibits the bands A and B of the Si (1 0 0) substrate and two additional peaks at 397 cm^{-1} (band C) and 568 cm^{-1} (band D), which are both due to ZnO [31]. Similar IR spectra were recorded for all growth times up to 40 h, the only difference between them being the peak area under each ZnO band, since this was found to decrease with increasing growth time.

For a better understanding of the growth mechanism, we examined and correlated the IR peaks obtained for various deposition times in a more systematic manner. The area under the peak was determined for each band as a function of time, using the FTIR spectrometer software, and is presented in Fig. 5. As can be seen, both band C (563–589 cm^{-1}) and band D (382–428 cm^{-1}) present the same basic trend: the area under the peaks significantly decreases with increasing growth time. For very short growth times (1–5 h) a dramatic decrease of the peak area is observed, followed by a period (10–30 h) where the peak area is almost constant. As an example, the peak area for the case of band D initially drops from 17.3 arbitrary units (1 h growth) to 7.9 arbitrary units (5 h growth); then, the peak area remains almost constant, at a value around 6.7

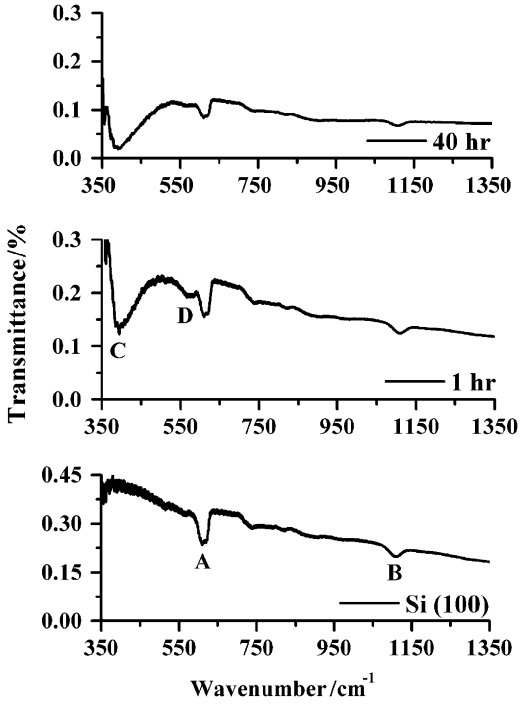

Fig. 4. IR spectra of ZnO grown by ACG at 95 °C for deposition times of 1 and 40 h. The IR spectrum of the Si (1 0 0) substrate used for the deposition is also shown.

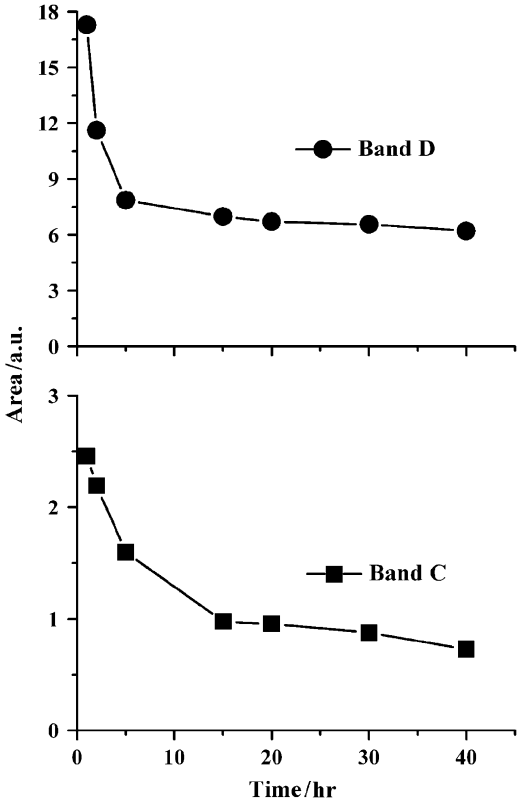

Fig. 5. Area under the peaks of the IR bands C and D of ZnO structures grown by ACG at 95 °C as a function of deposition time.

arbitrary units, at least for deposition time up to 30 h. For even longer growth times (40 h), the peak area further decreases (4.9 arbitrary units), indicating that there is less material present. It can be suggested that ZnO possibly dissolves away, affecting the sample's morphological characteristics (Fig. 3(c)).

In summary, the observed behaviour is a strong indication that for very short growth times (initial stage of the formation of ZnO structures), the production of ZnO is efficient. However, less ZnO is present as the deposition time increases.

Following the above experimental observations, single-phase ZnO is deposited for all growth times. A possible mechanism for ZnO growth can be considered in agreement with other researchers [20,32]. This mechanism involves the release and precipitation of formaldehyde (HCHO) (reaction 1), since there is no indication of its existence in the samples, followed by the hydrolysis of ammonia (NH_3) (reaction 2) and the production of $Zn(OH)_2$ (reaction 3), which finally gives ZnO and H_2O (reaction 4).

$$(CH_2)_6N_4 + 6H_2O \rightarrow 6HCHO + 4NH_3 \quad (1)$$

$$NH_3 + H_2O \leftrightarrow NH_4^+ + OH^- \quad (2)$$

$$Zn^{2+} + 2OH^- \leftrightarrow Zn(OH)_{2(l)} \quad (3)$$

$$Zn(OH)_{2(s)} \leftrightarrow ZnO_{(s)} + H_2O \quad (4)$$

Thus, it may finally be assumed from all the above analysis that for short deposition times the direction of reaction 4 is towards the right, indicating the completion of the reaction for 1–30 h to give ZnO. For even longer deposition times, the amount of ZnO is reduced, indicating that reaction 4 may be partially reversed to the left due to a process of ZnO formation and re-dissolution.

4. Conclusions

Kinetic studies of ZnO structures produced by ACG have been carried out. The effect of growth time on the structural and morphological characteristics of the samples has been investigated. XRD measurements have demonstrated that all the samples (1–40 h) are single-phase and have the ZnO hexagonal wurtzite structure. All growth periods show very good crystalline quality apart from the 40 h sample, indicating weak and broader peaks as illustrated by Raman spectroscopy. The morphology of the samples consists of flower-like structures and single rods, their size depending on growth time. It should be noticed that for 40 h growth the sample's morphology is different, with another space distribution of the structures observed. According to the FTIR studies performed, at short growth periods the ZnO production is more efficient, while for longer periods it decreases. The growth mechanism of ZnO seems to involve an interplay of deposition and re-dissolution processes.

Acknowledgements

The authors would like to thank Ms Mirela Suchea and Mrs Aleka Manousaki for SEM measurements.

References

[1] Y. Chen, D. Bagnall, T. Yao, Mater. Sci. Eng. B 75 (2000) 190.
[2] S. Liang, H. Sheng, Y. Liu, Z. Hio, Y. Lu, H. Shen, J. Crystal Growth 225 (2001) 110.
[3] M.H. Koch, P.Y. Timbrell, R.N. Lamb, Semicond. Sci. Technol. 10 (1995) 1523.
[4] C.R. Gorla, N.W. Emanetoglu, S. Liang, W.E. Mayo, Y. Lu, M. Wraback, H. Shen, J. Appl. Phys. 85 (1999) 2595.
[5] J.F. Chang, H.H. Kuo, I.C. Leu, M.H. Hon, Sensors Actuators B: Chem. 84 (2002) 258.
[6] H. Rensmo, K. Keis, J. Phys. Chem. B 101 (1997) 2598.
[7] E.M. Wong, P.C. Searson, Appl. Phys. Lett. 74 (1999) 2939.
[8] U. Ozgur, Y.I. Alivov, C. Liu, A. Teke, M.A. Reshchikov, S. Dogan, V. Avrutin, S.J. Cho, H. Morkoc, J. Appl. Phys. 95 (2005) 041301.
[9] W.-C. Shih, M.-S. Wu, J. Crystal Growth 137 (1994) 319.
[10] Y. Sun, G.M. Fuge, M.N.R. Ashfold, Chem. Phys. Lett. 396 (2004) 21.
[11] Y.W. Heo, V. Varadarajan, M. Kaufman, K. Kim, D.P. Norton, Appl. Phys. Lett. 81 (16) (2002) 3046.
[12] J.Q. Hu, X.L. Ma, Z.Y. Xie, N.B. Wong, C.S. Lee, S.T. Lee, Chem. Phys. Lett. 344 (2001) 97.
[13] J.J. Wu, S.C. Liu, Adv. Mater. 14 (2002) 215.
[14] B. Illy, B.A. Shollock, J.L. MacManus-Driscoll, M.P. Ryan, Nanotechnology 16 (2005) 320.
[15] S.A. Studenkin, N. Golego, M. Cocivera, J. Appl. Phys. 83 (1998) 2104.
[16] M. Ohyama, H. Kozuka, T. Yoko, Thin Solid Films 306 (1997) 78.
[17] L. Vayssieres, Adv. Mater. 15 (2003) 464.
[18] Q. Li, V. Kumar, Y. Li, H. Zhang, T.J. Marks, R.P.H. Chang, Chem. Mater. 17 (2005) 1001.
[19] X. Liu, Z. Jin, S. Bu, J. Zhao, K. Yu, Mater. Sci. Eng. B 129 (2006) 139.
[20] L. Vayssieres, Int. J. Nanotechnol. 1 (2004) 1.
[21] H. Zhang, D. Yang, S. Li, X. Ma, Y. Ji, J. Xu, D. Que, Mater. Lett. 59 (2005) 1696.
[22] G. Kenanakis, D. Vernardou, E. Koudoumas, G. Kiriakidis, N. Katsarakis, Sensors Actuators B: Chem., 2007, doi:10.1016/j.snb.2006.12.033.
[23] 〈http://www.ccp14.ac.uk〉.
[24] Z. Zhaochun, H. Baibiao, Y. Yongqin, C. Deliang, Mater. Sci. Eng. B 86 (2001) 109.
[25] R.P. Wang, G. Xu, P. Jin, Phys. Rev. B 69 (2004) 113303.
[26] A. Zwick, R. Carles, Phys. Rev. B 48 (1993) 6024.
[27] F. Decremps, J. Pellicer-Porres, A.M. Saitta, J.-C. Chervin, A. Polian, Phys. Rev. B 65 (2002) 092101.
[28] U. Steinike, W. Lutz, M. Wark, K. Jancke, Cryst. Res. Technol. 28 (1994) 149.
[29] M.C. Bernard, A. Hugot-Le Goff, D. Massinon, N. Phillips, Corros. Sci. 35 (1993) 1339.
[30] J. Lambers, P. Hess, J. Appl. Phys. 94 (2003) 2937.
[31] S. Musić, D. Dragčević, M. Maljković, S. Popović, Mater. Chem. Phys. 77 (2002) 521.
[32] S. Yamabi, H. Imai, J. Mater. Chem. 12 (2002) 3773.